Cubic Gold Nanoparticles Synthesis in the Presence of an Thioether Oligomer DDT-Poly(4-Vinylpyridine)

Fairouz Aberkane, Nadia Zine, Abdelhamid Errachid, Abdelhamid Elaissari

Cubic gold nanoparticles synthesis by in situ generation of seeds by chemical method in the presence of an oligomer thioether DDT-Poly(4-vinylpyridine)

*** Fairouz Aberkane[1,2], Nadia Zine[2], Abdelhamid Errachid[2] and Abdelhamid Elaissari[2]**

[1] *Faculty of Matter Science, Department of Chemistry, LCCE laboratory, University of Batna-1, 05000, Algeria*

[2] *Institute of Analytical Sciences (ISA), University Lyon, University of Claude Bernard Lyon-1, UMR 5280, 5 rue de la Doua, 69100 Villeurbanne, France*

* Corresponding author: fairouz.aberkane@univ-batna.dz

Abstract

In the present research work, we report a facile, in-situ, and seedless-based synthesis method of cubic gold nanoparticles at room temperature by using thioether oligomer ligand DDT-poly(4-vinylpyridine) as a functionalization and stabilization agent. Thioether oligomer ligand was synthesized by bulk radical polymerization in the presence of dodecanethiol, while, the synthesis of cubic gold nanoparticles was carried out by a reduction reaction by $NaBH_4$ in the presence of the pre-synthesized thioether oligomer ligand. The effect of stirring conditions on the growth of nanoparticles and their final morphology has been investigated. Synthesized thioether oligomer ligand and gold nanoparticles were thoroughly characterized using numerous techniques such as Size exclusion chromatography (SEC), Fourier transform infrared spectroscopy (FTIR), Proton nuclear magnetic resonance spectroscopy (^{1}H NMR), Transmission Electron Microscope (TEM), and UV–Visible spectroscopy.

Graphical abstract

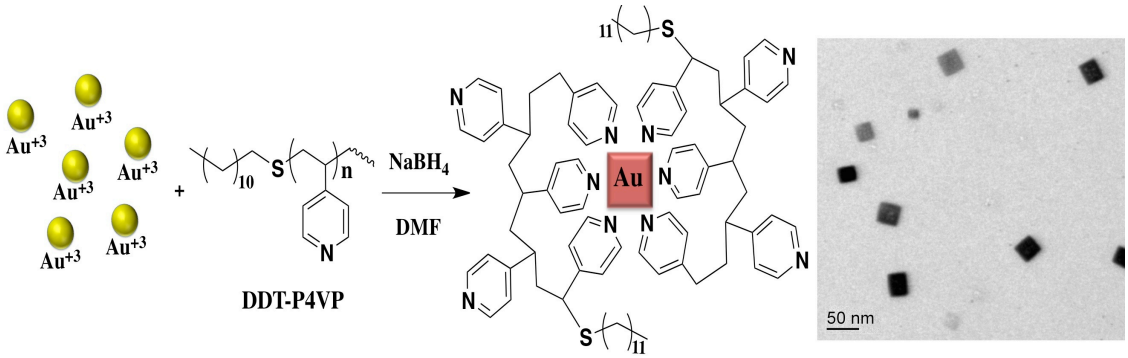

Keywords: *Poly(4-vinylpyridine), Cubic gold nanoparticles, Thioether oligomer, Dodecanethiol, Radical polymerization.*

1. Introduction

Anisotropic gold nanoparticles (AuNPs) are of increasing interest in many fields, because of their shape-dependent properties, in particular for medical fields [1][2][3]. These nanostructures have fascinating applications as photo-thermal therapy [4,5], drug delivery [6][7], biological imaging [8][9], chemical detection [10][11], and chemical catalysis [12][13]. Much effort on the development of new methodologies for the synthesis of anisotropic AuNPs has been provided over the last decade, in which the final reaction conditions of AuNPs synthesis have been optimized. Anisotropic AuNPs can be synthesized by seed and seedless methods, both strategies are classified as chemical methods, these methods allow better control of the size, morphology, and surface chemistry of nanoparticles, such as coating and functionalization [14][15]. In the seedless method, the nucleation and growth steps occurred at the same time, however, the seed-based method separates the nucleation and growth steps during the synthesis of nanoparticles by introducing small pre-synthesized core particles into a growth solution typically containing a metal precursor, a reducing agent, surfactant, and certain additives such as polymers [15]. Generally, polymers are used as functionalization and stabilization agents, in absence of stabilization the aggregation of nanoparticles causes the loss of their plasmonic properties and therefore their interesting applications [16]. The seed-based method has been demonstrated as a powerful synthetic route to generate a range of different anisotropic metal nanoparticles such as nanorods [17], nanoprisms [18], nanostars [19], and nanocubes [20].

Using Polymers in the nanoparticles synthesis process is very important; the dual role of polymer (functionalization and stabilization) in the synthetic method eliminates the need for an additional surfactant [21]. The combination of the properties of nanoparticles (e.g., optical) and macromolecules provides a possibility to prepare composite materials with unique properties compared to the individual nanoparticle and polymer [22][23]. Polymers containing functional groups with a high affinity for noble metal surfaces, and more especially thiol functionalities react with the AuNPs surfaces to form chemical interactions [24]. Sulfur-containing polymers, which carry functional groups at one end of a polymer chain, or in the middle, such as thioacetate [25], disulfide [26], thiol [27], and thioether[28], has been used for the synthesis of AuNPs. Polymer thioether ligands are widely used as polymeric stabilizers to prepare uniform metallic nanoparticles. Multiple

thioether-metal interactions can lead to stable and ordered monolayers on metal surfaces. They are a very useful system for the functionalization of nanoparticles for several applications [29][30]. The advantage of these products lies in their weak interactions with the surface of the nanoparticles, which allows them to be easily replaced by other ligands [29]. In comparison with other approaches using polymers as stabilizing and functionalizing agents, thioether polymers lead to the formation of nanoparticles of spherical morphology, which exhibit a significantly uniform monodispersity with small particle size. Xin Huang, et al. describe an approach to generate spherically and fairly uniform AuNPs with diameters about 2 – 6 nm using thioether end-functional polymer ligands dodecanethiol (DDT)-poly(vinyl acetate) as the stabilizing agents [31]. Wang et al. reported a one-step aqueous preparation of highly monodisperse AuNPs with diameters less than 5 nm using thioether-functionalized polymer ligands: DDT-poly(acrylic acid), DDT-poly(methacrylic acid), DDT-poly(vinylsulfonic acid), DDT-poly(vinylpyrrolidone), DDT-poly(hydroxyethyl acrylate), and DDT-poly(ethyleneglycol methacrylate) [32].

In the present work, cubic AuNPs were synthesized by a seedless method using a pre-synthesized oligomer containing a thioether functionality in its chains, DDT-Poly(4-vinylpyridine). In this method nucleation and growth of nanoparticles are produced in a single phase in an organic medium (DMF) at room temperature. The effect of stirring conditions on the growth of nanoparticles and their final morphology has been investigated. Using measurements by SEC, ^{1}H NMR, FTIR, TEM, UV-Visible spectroscopy, synthesized products; thioether oligomer ligand and AuNPs have been characterized.

2. Materials and methods

2.1. Materials

4-Vinylpyridine (4VP, ≥95%); Tetrachloroauric acid ($HAuCl_4.3H_2O$, 99.999%); Dimethylformamide (DMF, ≥99.8%) and Hexane (≥95%) were purchased from Sigma-Aldrich. 1-Dodecanethiol (DDT, >97%) and benzoyl peroxide (BPO, >97%) were obtained from Fluka. Sodium tetrahydroborate ($NaBH_4$ 98%) and diethyl ether (99,5%) were obtained from Riedel-deHaën. All reagents were used as obtained except monomer and initiator; 4VP was purified by vacuum distillation (colorless liquid was obtained) and BPO was purified via the recrystallization process in Methanol.

2.2. Experimental methods

Size exclusion chromatography (SEC) was used to determine the average weight and the polydispersity index of the prepared oligomer. An AGILENT 1200 series isocratic pump equipped with an AGILENT 1200 series automatic switch and a set of columns, was used for the analyzes. Detection was performed by an AGILENT 1260 Infinity refractometer. A PC driver set and retreat the results using two software programs: Agilent Chemstation (for pump control) and Astra V version 5.3.4.14 (to acquire and interpret the results). The infrared spectrum of synthesized thioether oligomer was recorded on Nexus 470 FTIR spectrometer in a total Reflexing attenuated on Crystal of Diamond in mono-reflexion (Smart-orbit, Thermo Scientific). The spectral range is from 4000 to 400 cm^{-1}, with 256 scans and 4 cm^{-1} of resolution. The detector is a DTGS (Deuterated Tri-Glycine Sulfate). A Bruker AV400 MHz spectrometer was used to recorde ^{1}H NMR spectrum. Analysis was carried out in DMSO at room temperature using the δ scale and tetramethylsilane (TMS) as an internal standard. The chemical shift were given in ppm relative to tetramethylsilane. UV–Visible characterization of AuNPs dispersions was performed using a UV–Visible spectrophotometer (UV-1700, Shimadzu). The absorbance measurements were made over the wavelength range of 400-700 nm using 1 cm path length quartz cuvettes. Transmission Electron Microscopy (TEM) was performed with a Philips CM120 microscope. A droplet of the suspension was deposited on a microscope grid (copper support covered with carbon) and slowly dried in open air. The dry samples were observed by TEM under 100 kV acceleration voltages.

3. Experimental

3.1. Synthesis of functional thioether oligomer ligand

Oligomer synthesis reaction was carried out as described previously [33]; 2 mL of monomer (4VP, 18.83 mmol), 1.2 mL of Dodecanethiol (DDT, 5 mmol), and 10 mg of benzoyl peroxide (BPO, 0.0413 mmol) were mixed. The mixture was degassed for 30 min using an ultrasonic apparatus to remove the oxygen dissolved in the solution, then placed in a pre-heated oil bath. The temperature of the reaction mixture was maintained between 100-110˚C and heated for 48 h. After cooling, viscous product, red in color, was obtained. The synthesized oligomer was isolated by dissolving the reaction mixture in methanol and precipitating it into diethyl ether. This step was repeated several times for removing the

unreacted monomer. Oligomer thus obtained was dried, at ambient temperature, then at 50˚C to a constant weight. The yield of the obtained thioether oligomer DDT–P4VP was 55.62%.

3.2. Preparation of cubic AuNPs using thioether oligomer ligand

Cubic AuNPs, stabilized by oligomeric thioether ligands, were synthesized according to the following method; firstly, all glassware was rinsed with aqua regia (HNO_3/HCl: 1V/3V) and several times with Milli-Q water. Afterward, 45.2 mg of the oligomer (DDT-P4VP) was introduced in 10 mL of $HAuCl_4$ solution (1 mM in DMF). The reaction mixture was stirred with a magnetic stir for 24 h in dark conditions. The reduction reaction of Au^{+3} ions is carried out by the dropwise addition, under stirring (700 rpm), of 1 mL of a freshly prepared aqueous solution of $NaBH_4$ (0.1 M). The solution color changed from pale yellow to dark with a deep purple to a red color indicating the formation of AuNPs. Thereafter, stirring is stopped and the solution is kept in the dark for complete growth of the cubic AuNPs. Finally, the prepared nanoparticles were purified by centrifugation (at 10.000 rpm) and redispersed in DMF.

4. Results and discussion

4.1. Synthesis and characterization of thioether oligomer ligand

The DDT-4NVP thioether oligomer was synthesized by the process of radical bulk polymerization of 4VP in the presence of DDT as a chain transfer agent (Scheme 1). The polymerization reaction is initiated by a thermal initiator (BPO) at a temperature between 100 − 110 ˚C for 48 hours. In reality, DDT also can contribute to the initiation of polymerization; sulfur has a high affinity with radicals and can easily lose the hydrogen from thiol by transfer reaction and give rise to the formation of the sulfide radical. The reactive fragments resulting from the decomposition of DDT can also initiate polymer chains [32][33]. Since the amount of DDT is much higher compared to the initiator (BPO), the initiation comes mainly from thiol fragments. The molecular weight of the DDT-P4VP oligomers was determined using size exclusion chromatography (SEC). The weight average molecular mass (Mw) of DDT-P4VP was 745 g/mol compared to standard polystyrene, with a polydispersity index of 1.06. The calibration is carried out with four standard polystyrenes of increasing masses (380, 1020, 1860, 2698 g/mol). However, the slightly narrow molecular

weight distributions, are due to the radical polymerization technique used which greatly resembles controlled radical polymerization. Also, the molecular weight of 4VP is 105.14 g/mol, which means that the degree of polymerization of the obtained oligomer is approximately 5.

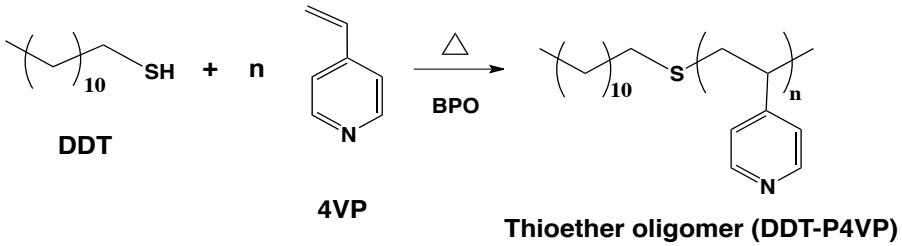

Scheme 1. Polymerization reaction of 4VP in the presence of DDT.

The FTIR-ATR spectroscopy was used to characterize the structure of oligomer ligand DDT–P4VP. In the spectrum of DDT-P4VP presented in Figure 1, the absorption peaks at 1598, 1557, and 1415 cm^{-1} can be assigned to the ring vibration of pyridine in P4VP. The bands at 1557 and 1415 cm^{-1} were attributed to the stretching vibration absorption of aromatic C–C bonds while the band at 1598 cm^{-1} was attributed to the absorption of aromatic and conjugated C=C bonds. The band in the spectrum of P4VP around 1220.11 cm^{-1} is the stretching vibration absorption of C–N bond. The monomer units of P4VP corresponding to the ring deformation appear around 993 - 994 cm^{-1}. Bands around 2853 and 2927 cm^{-1} correspond to the aliphatic C–H absorption coming from oligomer and DDT fragment. Moreover, the presence of peaks at around 2800–3100 cm^{-1} corresponds to the aromatic and aliphatic C–H stretching in DDT-P4VP.

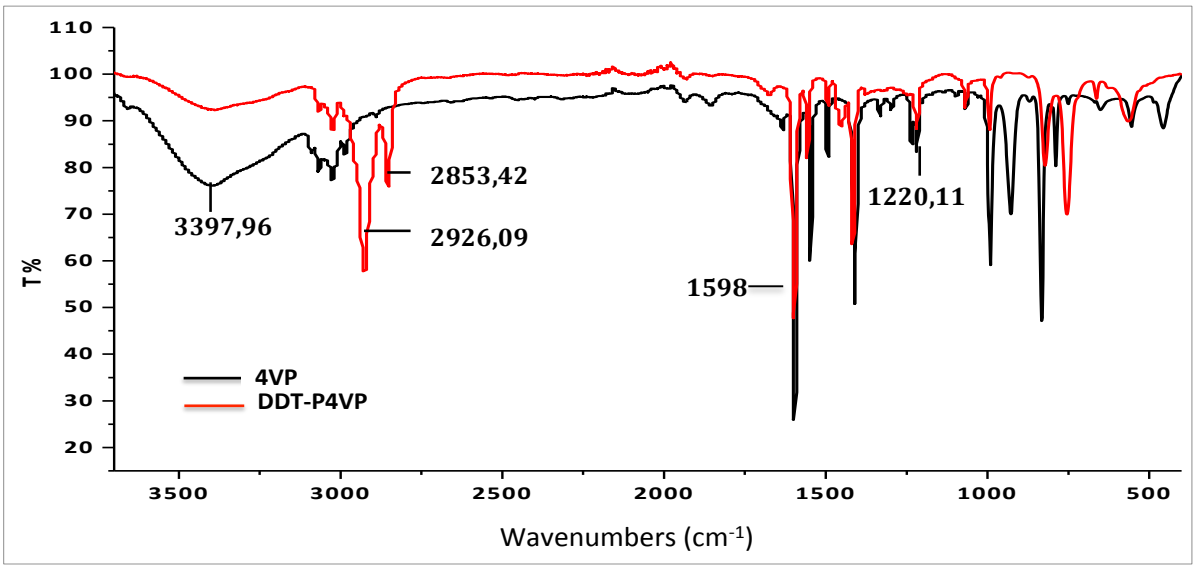

Figure 1. FTIR spectra of 4VP and the obtained DDT-P4VP polymer.

The ^{1}H NMR spectrum of DDT-P4VP is shown in Figure 2. Proton peaks presented at δ = 8.27 and 6.59 ppm correspond to the H_7 and H_6 protons of pyridinium group in 4VP, respectively, the main chain methine (H_5) and methylene protons (H_4) are assigned in the range of 1.32–1.77 ppm [34]. Signals located at 0.84, 1.22, and 2.52 ppm are attributed to the aliphatic protons of the DDT fragment, linked to the chain end of the oligomer, H_1, H_2 and H_3 respectively [35]. Both the FTIR and ^{1}H NMR spectra indicated that the synthesis of DDT-P4VP was accomplished successfully.

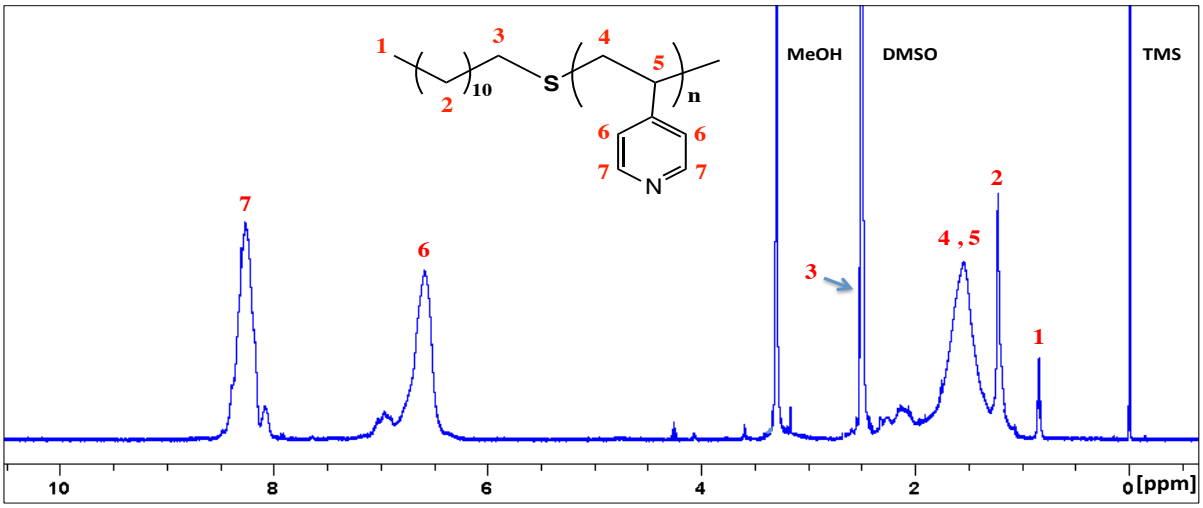

Figure 2. ^{1}H NMR spectrum of synthesized thioether oligomer DDT-P4VP.

4.2. Preparation and characterization of cubic AuNPs

Thioether oligomer was synthesized, by the bulk radical polymerization method, in the presence of a transfer agent (DDT). The use of the transfer agent was to have sulfur in the oligomer chain; sulfur can produce interactions with the surface of AuNPs because of its affinity with noble metals [36][37]. In this part, we report the synthesis and functionalization of AuNPs in an organic medium (in DMF). The selected solvent is a good solvent for gold salt and the oligomer ligand. Here, the DMF solvent is miscible with water, so both solutions of the reducing agent and gold ions form a single phase. The functionalization of the AuNPs was carried out during synthesis by introducing the oligomer into the reaction mixture (Scheme 2). The presence of several nitrogen atoms along the polymer chain, in the pyridine moieties more than sulfur atoms, leads us to think that several contact points between the nitrogen atoms and the nanoparticles can be formed and help the oligomer to attach to the surface of the nanoparticles after reduction reaction.

These pyridine moieties can create multiple interactions on the surface of the metal and lead to electrostatic and steric stabilization [38] as shown in scheme 2.

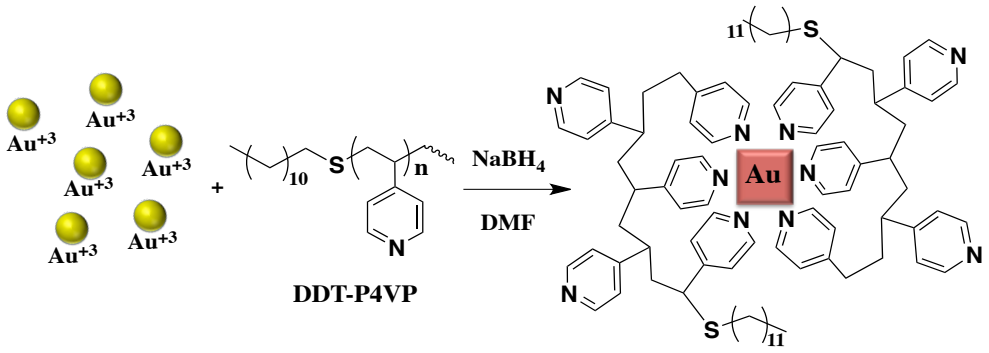

Scheme 2: Cubic AuNPs synthesis reaction with the proposed morphology of the obtained DDT-P4VP stabilized AuNPs.

In general, the mechanism of nanoparticles formation passes through successive steps of nucleation and growth. Several parameters are responsible for the final shape of nanoparticles. At the growth step, stabilizers, surfactants, shaping agents, and growth kinetics determine the final shapes of the resulting nanoparticles. The TEM image (Figure 4) shows the presence of cubic-shaped nanoparticles in addition to small spherical-shaped nanoparticles, which confirms that the nucleation of nanoparticles begins with the formation of spherical nuclei, and the growth of nanoparticles, under specific conditions, leads to the formation of cubic AuNPs. Without stirring and in the presence of an oligomer, that has pyridine fragments, helps the growth of the spherical nanoparticles into cubic nanoparticles. This phenomenon is noticed, likewise, in the case of gold nanorods synthesis, which requires that the stiring be suspended after the addition of the reducing agent to promote the growth and progression of the nanorods in a single dimension. The mean diameter of the obtained cubic AuNPs and its polydispersity index (PDI) were calculated by averaging over 90 particles from the TEM images using ImageJ software, the average diameter is 47.95 nm with a PDI equal to 0.3. The obtained AuNPs are cubic in shape and relatively uniform. Consequently, thioether oligomer ligand DDT-P4VP acts simultaneously as a stabilizing and shaping agent.

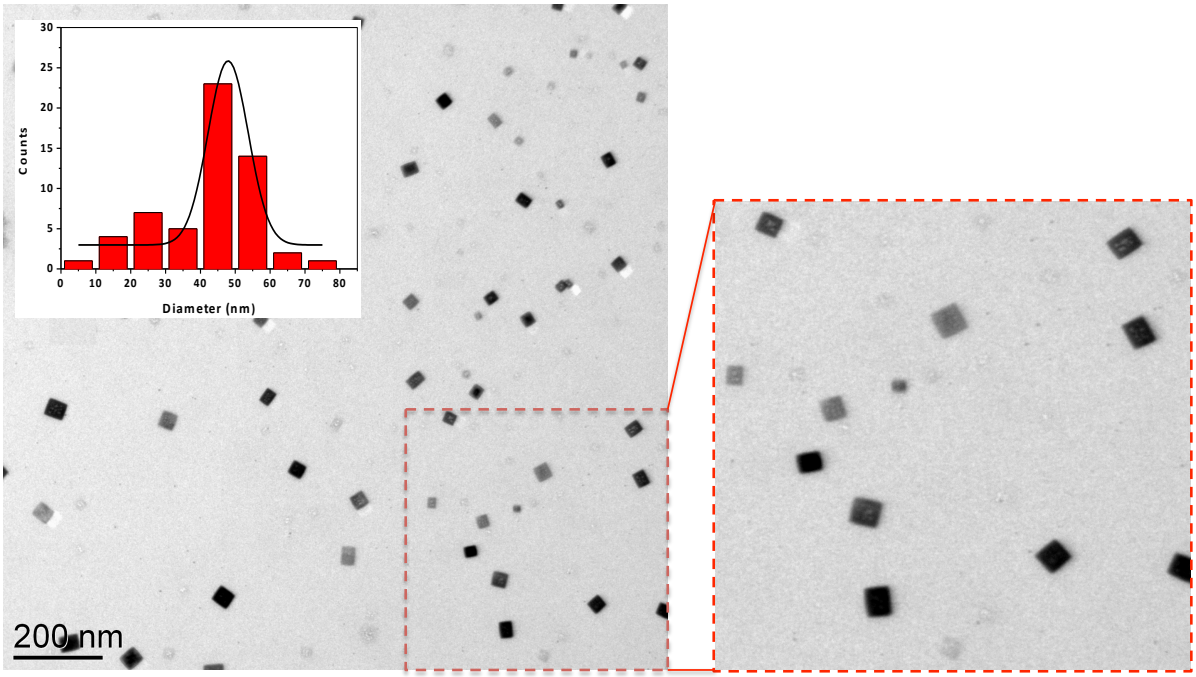

Figure 4. TEM image of cubic AuNPs prepared using thioether oligomer ligand DDT-P4VP.

Small, spherical, and fairly uniform AuNPs were obtained using the same thioether oligomer DDT-P4VP. The reaction was carried out under the same conditions used for the synthesis of cubic AuNPs except the stirring condition; the reaction mixture was stirred continuously overnight at 700 rpm. The TEM image presented in figure 5, shows spherical-shaped nanoparticles, the mean diameter, and the polydispersity index (PDI) of the obtained AuNPs were calculated by averaging over 568 particles from the TEM image. The average diameter of the obtained AuNPs is 3.55 nm with a PDI equal to 0.22, the obtained AuNPs are relatively uniform.

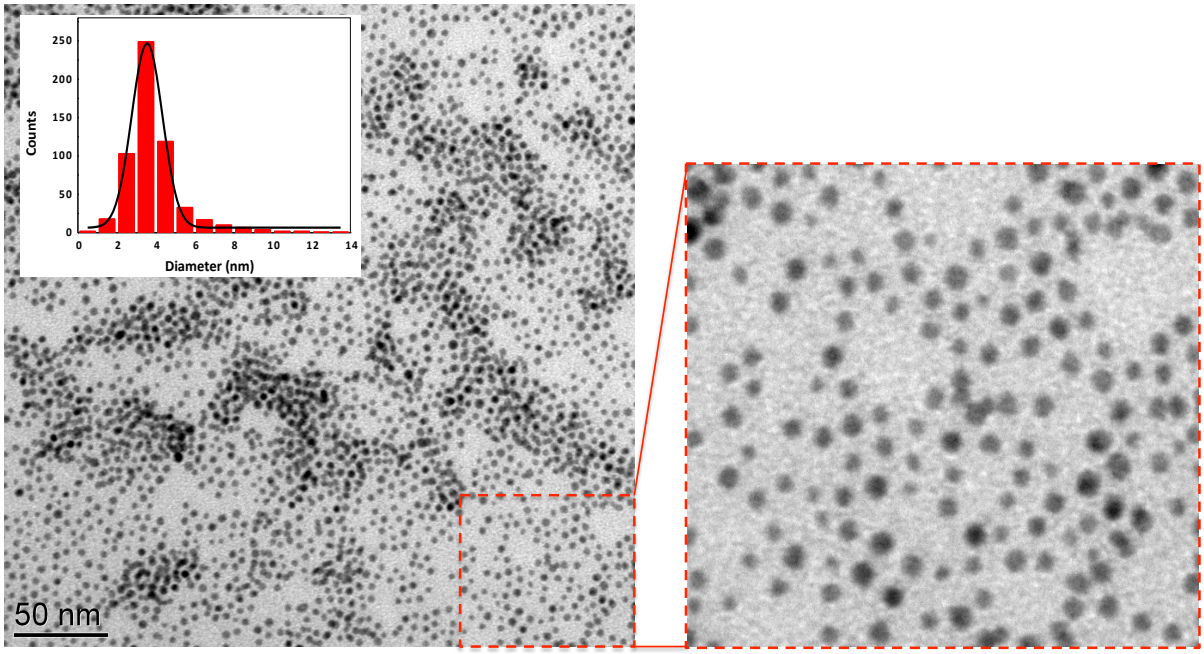

Figure 5. TEM images of spherical AuNPs prepared in presence of thioether oligomer ligand DDT-P4VP.

The interaction of AuNPs with light leads to a phenomenon called surface plasmon resonance (SPR), which results in strong absorption in the visible region between 500 nm and 800 nm depending on the size and shape of the nanoparticles, which can be measured by UV-Visible spectroscopy. The UV-Visible spectrum of the resulting cubic AuNPs presented in Figure 6 shows a distinct plasmon resonance peak. The maximum wavelength (λmax) was found at 551.43 nm, this wavelength is well within the range generally observed for cubic-shaped AuNPs [39][40]. However, the UV-Visible spectrum of the obtained spherical AuNPs (Figure 6) shows an intense absorption peak at 517 nm. Optical properties such as absorption maxima and absorption intensity usually depend on the size of the nanoparticles. An intense absorption peak is, in general, attributed to the surface plasmon excitation of small spherical particles [41].

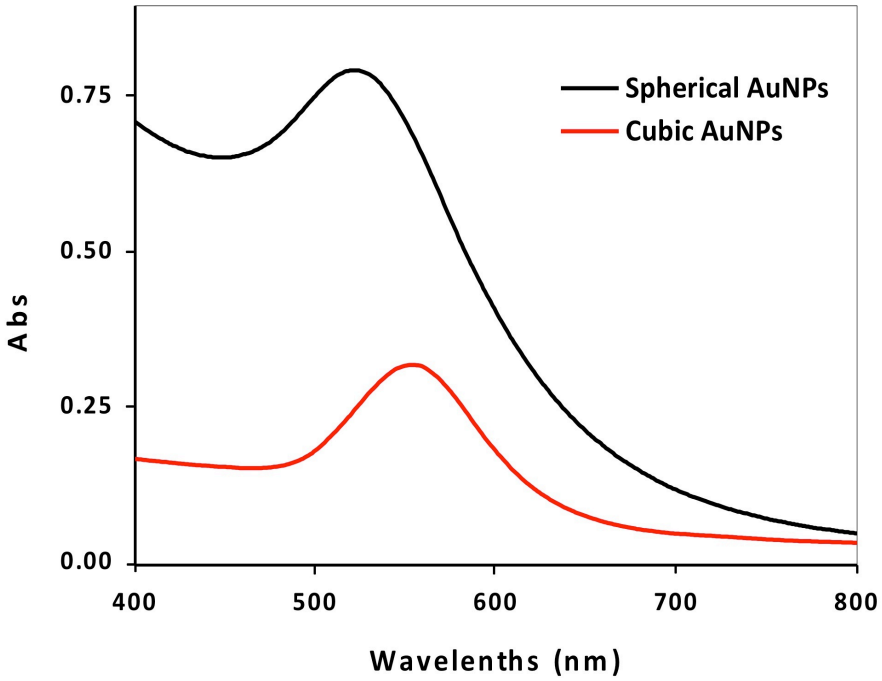

Figure 6. UV-Visible absorption spectra of cubic AuNPs and spherical AuNPs prepared in presence of DDT-P4VP oligomeric ligand in DMF.

5. Conclusion

In this work, an oligomeric ligand containing thioether function in its chain (DDT-P4VP) was synthesized and used as a functionalization and stabilization agent for AuNPs. Thioether oligomer ligand was synthesized by bulk radical polymerization in the presence of dodecanethiol, while, the synthesis of AuNPs was carried out using seedless-based synthesis method, by a reduction reaction in an organic medium (DMF) and at room temperature. The effect of the stirring condition on the growth of nanoparticles and their final morphology has been studied. The obtained results showed that stirring condition is an important factor to obtain a specific shape; synthesis reaction with a continuous stirring involves spherical-shaped AuNPs with fairly uniform and small size (3.55 nm), however, without stirring cubic AuNPs with a relatively large size (47 nm) were obtained. These results indicate that the thioether oligomeric ligand DDT-P4VP can act as a shaping agent for AuNPs. Synthesized thioether oligomer ligand and AuNPs were thoroughly characterized using numerous techniques such as SEC, FTIR, ^{1}H NMR, TEM, and UV-Visible spectroscopy.

References

[1] C.J. Murphy, T.K. Sau, A.M. Gole, C.J. Orendorff, J. Gao, L. Gou, S.E. Hunyadi, T. Li, Anisotropic Metal Nanoparticles : Synthesis , Assembly , and Optical Applications, (2005) 13857–13870.

[2] Y. Hua, K. Chandra, D.H.M. Dam, G.P. Wiederrecht, T.W. Odom, Shape-Dependent Nonlinear Optical Properties of Anisotropic Gold Nanoparticles, (2015) 4904–4908. doi:10.1021/acs.jpclett.5b02263.

[3] C. Kohout, C. Santi, Anisotropic Gold Nanoparticles in Biomedical Applications, (2018). doi:10.3390/ijms19113385.

[4] W. Yingxin, Z. Qianqian, Preparation of novel anisotropic gold nanoplatform as NIR absorbing agents for photothermal therapy of liver cancer and enhanced ultrasound contrast imaging Preparation of novel anisotropic gold nanoplatform as NIR absorbing agents for photothermal therapy of liver cancer and enhanced ultrasound contrast imaging, (2020).

[5] Q.I.N.C. Hen, Y.A.R. En, Anisotropic scattering characteristics of nanoparticles in different morphologies : improving the temperature uniformity of tumors during thermal therapy using forward scattering, 12 (2021) 893–906.

[6] A. Brandelli, Bioactivity of noble metal nanoparticles decorated with biopolymers and their application in drug delivery, Elsevier B.V. (2015). doi:10.1016/j.ijpharm.2015.10.059.

[7] A.V. Singh, M. Batuwangala, R. Mundra, K. Mehta, S. Patke, E. Falletta, R. Patil, W.N. Gade, Biomineralized Anisotropic Gold Microplate − Macrophage Interactions Reveal Frustrated Phagocytosis-like Phenomenon : A Novel Paclitaxel Drug Delivery Vehicle, (2014).

[8] Y. Peng, B. Xiong, L. Peng, H. Li, Y. He, E.S. Yeung, Recent Advances in Optical Imaging with Anisotropic Plasmonic Nanoparticles Recent Advances in Optical Imaging with Anisotropic Plasmonic Nanoparticles, (2014). doi:10.1021/ac504061p.

[9] Background-Free Imaging of Viral Capsid Proteins- Coated Anisotropic Nanoparticle on Living Cell Membrane with Dark-Field Optical Microscopy, (2017). doi:10.1021/acs.analchem.7b03762.

[10] A. Manuscript, Materials Chemistry C, (n.d.). doi:10.1039/x0xx00000x.

[11] L. Jin, C. Han, Sensors and Actuators B : Chemical Eco-friendly colorimetric detection of mercury (II) ions using label-free anisotropic nanogolds in ascorbic acid solution, Sensors Actuators B. Chem. 195 (2014) 239–245. doi:10.1016/j.snb.2014.01.020.

[12] T. Premkumar, K. Lee, K.E. Geckeler, Shape-tailoring and catalytic function of anisotropic gold nanostructures, (2011) 1–12.

[13] G.P. Sahoo, S. Basu, S. Samanta, A. Misra, Microwave-assisted synthesis of anisotropic gold nanocrystals in polymer matrix and their catalytic activities, J. Exp. Nanosci. 10 (2015) 690–702. doi:10.1080/17458080.2013.877163.

[14] N. Li, P. Zhao, D. Astruc, Anisotropic Gold Nanoparticles : Synthesis , Properties , Applications , and Toxicity Angewandte, (2014) 1756–1789. doi:10.1002/anie.201300441.

[15] J.E. Ortiz-castillo, R.C. Gallo-villanueva, M.J. Madou, V.H. Perez-gonzalez, Anisotropic gold nanoparticles : A survey of recent synthetic methodologies, Coord. Chem. Rev. 425 (2020) 213489. doi:10.1016/j.ccr.2020.213489.

[16] C. Saldías, S. Bonardd, C. Quezada, D. Radi, A. Leiva, The Role of Polymers in the

Synthesis of Noble Metal Nanoparticles : A Review, 17 (2017) 87–114. doi:10.1166/jnn.2017.13016.
[17] A. Gole, C.J. Murphy, Seed-Mediated Synthesis of Gold Nanorods : Role of the Size and Nature of the Seed, (2004) 3633–3640.
[18] B.J.E. Millstone, G.S. Métraux, C.A. Mirkin, Controlling the Edge Length of Gold Nanoprisms via a Seed-Mediated Approach **, (2006) 1209–1214. doi:10.1002/adfm.200600066.
[19] M.M. Phiri, D.W. Mulder, Seedless gold nanostars with seed-like advantages for biosensing applications, (2019) 0–9.
[20] M. Thiele, J. Zi, E. Soh, A. Knauer, D. Malsch, O. Stranik, R. Müller, A. Csáki, T. Henkel, J.M. Köhler, W. Fritzsche, Gold nanocubes – Direct comparison of synthesis approaches reveals the need for a microfluidic synthesis setup for a high reproducibility, Chem. Eng. J. 288 (2016) 432–440. doi:10.1016/j.cej.2015.12.020.
[21] J. Shan, H. Tenhu, Recent advances in polymer protected gold nanoparticles : synthesis , properties and applications, (2007) 4580–4598. doi:10.1039/b707740h.
[22] C.K. Adokoh, S. Quan, M. Hitt, J. Darkwa, P. Kumar, R. Narain, Synthesis and evaluation of glycopolymeric decorated gold nanoparticles functionalized with gold-triphenyl phosphine as anti-cancer agents, Biomacromolecules. 15 (2014) 3802–3810. doi:10.1021/bm5010977.
[23] H. Banu, D. Kaur, A. Edgar, A. Sheriff, N. Rayees, N. Renuka, S.M. Faheem, K. Premkumar, G. Vasanthakumar, Journal of Photochemistry and Photobiology B : Biology Doxorubicin loaded polymeric gold nanoparticles targeted to human folate receptor upon laser photothermal therapy potentiates chemotherapy in breast cancer cell lines, J. Photochem. Photobiol. B Biol. 149 (2015) 116–128. doi:10.1016/j.jphotobiol.2015.05.008.
[24] X. Zhou, J.M. El Khoury, L. Qu, L. Dai, Q. Li, A facile synthesis of aliphatic thiol surfactant with tunable length as a stabilizer of gold nanoparticles in organic solvents, J. Colloid Interface Sci. 308 (2007) 381–384. doi:10.1016/j.jcis.2007.01.040.
[25] D. González-Fernández, M. Torneiro, M.A. López-Quintela, M. Lazzari, Copolymers with acetyl-protected thiol pendant groups as highly efficient stabilizing agents for gold surfaces, RSC Adv. 5 (2015) 13722–13726. doi:10.1039/C4RA12458H.
[26] J. Boudon, M. Vonlanthen, T. Scharf, Liquid-Crystalline Thiol- and Disulfide-Based Dendrimers for the Functionalization of Gold Nanoparticles, (2009) 2321–2337.
[27] B. Jang, J.Y. Park, C.H. Tung, I.H. Kim, Y. Choi, Gold nanorod-photosensitizer complex for near-infrared fluorescence imaging and photodynamic/photothermal therapy in vivo, ACS Nano. 5 (2011) 1086–1094. doi:10.1021/nn102722z.
[28] I. Hussain, S. Graham, Z. Wang, B. Tan, C. David, S.P. Rannard, A.I. Cooper, M. Brust, D.C. Sherrington, Size-Controlled Synthesis of Near-Monodisperse Gold Nanoparticles in the 1 − 4 nm Range Using Polymeric Stabilizers Size-Controlled Synthesis of Near-Monodisperse Gold Nanoparticles in the 1-4 nm Range Using Polymeric Stabilizers, (2005) 16398–16399. doi:10.1021/ja055321v.
[29] S. Razzaque, S.Z. Hussain, I. Hussain, B. Tan, Design and utility of metal/metal oxide nanoparticles mediated by thioether end-functionalized polymeric ligands, Polymers (Basel). 8 (2016). doi:10.3390/polym8040156.
[30] Y. Niu, R.M. Crooks, Dendrimer-encapsulated metal nanoparticles and their applications to catalysis, 6 (2003) 1049–1059. doi:10.1016/j.crci.2003.08.001.
[31] X. Huang, B. Li, H. Zhang, I. Hussain, L. Liang, B. Tan, Facile preparation of size-

controlled gold nanoparticles using versatile and end-functionalized thioether polymer ligands, Nanoscale. 3 (2011) 1600–1607. doi:10.1039/C0NR00835D.
[32] Z. Wang, B. Tan, I. Hussain, N. Schaeffer, M.F. Wyatt, M. Brust, A.I. Cooper, S.U. V, S. Park, U. Kingdom, R. V September, Design of Polymeric Stabilizers for Size-Controlled Synthesis of Monodisperse Gold Nanoparticles in Water, (2007) 885–895.
[33] F. Aberkane, A. Barakat, A. Elaissari, N. Zine, T. Bendaikha, Electrochemical Sensor Based on Thioether Oligomer Poly (N-vinylpyrrolidone) -modified Gold Electrode for Bisphenol A Detection, (2019) 2112–2119. doi:10.1002/elan.201900060.
[34] C. Huang, S. Kuo, J. Chen, F. Chang, Synthesis and Characterization of Polystyrene-b-Poly (4-vinyl pyridine) Block Copolymers by Atom Transfer Radical Polymerization Synthesis and Characterization of Polystyrene-b-Poly (4-vinyl pyridine) Block Copolymers by Atom Transfer Radical Polymerization, (2005). doi:10.1007/s10965-004-5665-2.
[35] J. Jayabharathi, G.A. Sundari, V. Thanikachalam, P. Jeeva, S. Panimozhi, RSC Advances, RSC Adv. 7 (2017) 38923–38934. doi:10.1039/C7RA07080B.
[36] H. Häkkinen, The gold-sulfur interface at the nanoscale, Nat. Chem. 4 (2012) 443–455. doi:10.1038/nchem.1352.
[37] M. Tachibana, K. Yoshizawa, A. Ogawa, H. Fujimoto, R. Hoffmann, Sulfur-gold orbital interactions which determine the structure of alkanethiolate/Au(111) self-assembled monolayer systems, J. Phys. Chem. B. 106 (2002) 12727–12736. doi:10.1021/jp020993i.
[38] J. Li, L. Shi, Y. An, Y. Li, X. Chen, H. Dong, Reverse micelles of star-block copolymer as nanoreactors for preparation of gold nanoparticles, Polymer (Guildf). 47 (2006) 8480–8487. doi:10.1016/j.polymer.2006.09.071.
[39] A. Journal, L. Adorno, M. Cordero, C. Vélez, I. Feliciano, C. Cabrera, Biosynthesis of Gold Nanoparticles using Osmudaria Obtusiloba Extract and their Potential use in Optical Sensing Applications, 1 (2015) 1–9.
[40] Y. Chen, X. Gu, C. Nie, Z. Jiang, Z. Xie, C. Lin, Shape controlled growth of gold nanoparticles by a solution synthesis Shape controlled growth of gold nanoparticles by a solution synthesis, (2005). doi:10.1039/b504911c.
[41] M.A.K. Abdelhalim, M.M. Mady, M.M. Ghannam, Physical Properties of Different Gold Nanoparticles : Ultraviolet-Visible and Fluorescence Measurements Nanomedicine & Nanotechnology, 3 (2012). doi:10.4172/2157-7439.1000133.